Desalination and Water Treatment
www.deswater.com

doi: 10.5004/dwt.2019.23627

146 (2019) 266–277
April

Arsenite removal mechanism from groundwater in a two-dimensional batch electrochemical treatment process

Murthy Shruthi*, Shivaswamy Mahesh, Mahesh Sahana, Hanumanthappa Srikantha

Department of Environmental Engineering, SJCE (JSS S&T University), Mysuru, India-570006,
emails: shruthimvj@gmail.com (M. Shruthi), maheshs@sjce.ac.in (S. Mahesh), sahanam@sjce.ac.in (M. Sahana),
sriki.env@gmail.com (H. Srikantha)

Received 13 June 2018; Accepted 13 December 2018

ABSTRACT

This research work presents treatment of arsenite contaminated groundwater using batch electrochemical coagulation process using iron electrodes. The influence of various operating conditions was studied for applied cell voltages 6, 8, 12, and 16 V and specific surface area/volume ratio 40, 60, and 100 m^2/m^3 for electrolysis time (ET) of 60 min with constant initial $As(III)_0$ of 3 mg/L. The focus was to decrease arsenic concentration to the prescribed drinking water quality standards, to exercise water quality control of other parameters after electrochemical treatment (ECT), to optimize anode dissolution, to control sludge volume, to lower the energy consumption and to minimize operating cost. The operating conditions were pre-set with an intent to retain the water mineral content after ECT. For the optimal operating conditions of 16 V 4 electrodes (4E - 4 no. of Fe electrodes) arrangement, As(III) was reduced from 3 to 0 mg/L in a shortest ET of 10–15 min with electrode dissolution 0.7838 kg/m^3, dry sludge 1.21 kg/m^3, energy consumption 0.397 KWh/m^3 with a corresponding operating cost of INR 1.15/m^3, such a low cost was because the operating conditions were established in this work. Thus, ECT proved as an effective and efficient treatment technology for arsenic (III) removal from groundwater.

Keywords: Arsenite; Iron electrodes; Applied cell voltage; Number of electrodes; Anode dissolution; Energy consumption

1. Introduction

Lack of safe and potable drinking water is a global challenge for billions of people living in developing countries. Acidic conditions of precipitation run-off and long residence time of water in the aquifer renders the groundwater toxic. Anthropogenic activities from non-point sources such as water percolation from mining areas, agricultural chemicals and discharge from free mining activities and metallurgical industry contribute to increased arsenic levels in water [1–3]. Arsenic contamination of groundwater in West Bengal basin in India is one of the worst natural geo-environmental disasters till date [4]. An estimated 6 million people in West Bengal are exposed to arsenic levels of 0.05–3.2 mg/L [5]. Arsenic concentrations in groundwater exceed permissible limits (0.05 mg/L) in parts of Assam in 20 of 24 districts, 3 of 4 districts in Tripura, 6 of 13 districts in Arunachal Pradesh, 2 of 8 districts in Nagaland, and 1 of 9 districts in Manipur [6]. Also, some areas adjoining Chandigarh have high arsenic levels of over 5.45 mg/L in bore wells fitted with hand-pump. Because of its high toxicity, the United States Environmental Protection Agency and World Health Organization (WHO) limit the maximum contaminant levels in drinking water of 50–10 μg/L. Arsenic exists in groundwater as Arsenite (As(III)) and Arsenate (As(V)). Arsenite is predominant in anaerobic groundwater, 25–60 times more toxic than As(V) [7]. Arsenic cannot be easily destroyed, but can only be converted into different forms or transformed into insoluble compounds in combination with other elements such as iron [8–11]. The speciation of arsenic [As(III) and As(V)] and

---

* Corresponding author.

chromium [Cr(III) and Cr(VI)] was carried out by high performance liquid chromatography [12,13].

Conventional arsenic removal technologies include coagulation, adsorption, membrane technique and nano-filtration. Coagulation [14], precipitation [15] and other adsorption techniques using activated alumina [16], activated carbon [17] and ion exchange processes [18] are efficient in removing As(V) but are ineffective for As(III) removal. Multi-walled carbon nanotubes remove arsenate and arsenite by 92% and 91% [19]. The best removal occurs at pH 5–8 for 2–5 mg/L concentration of arsenate at 3 volts of current after 12 min EC processing time [20]. Among various water purification and recycling technologies, adsorption is quick, inexpensive, and universal method [21–23] for lower arsenic concentrations. With the revision of the permissible levels to 0.01 mg/L by WHO guidelines in 1993 [24], it is necessary to investigate novel treatment approaches that consistently provide drinking water with arsenic levels <0.01 mg/L. The aforesaid conventional treatment methods have many drawbacks such as generation of a considerable quantity of secondary pollutants, high sludge generation, inefficient and ineffective contaminant removal. These drawbacks demand finding cost effective, novel and quick alternate treatment technologies for arsenic removal to <0.01 mg/L in a short treatment time.

Electrochemical coagulation (ECC) is a novel treatment option for reducing the treatment time much lesser than the conventional treatment methods. ECC being simple with two dimensional (2D) infrastructure or three dimensional (3D) sacrificial metal anode faces offer multitude advantages and very useful in small and remote communities with no grid power to operate an ECC system. Solar power may be harnessed through solar panels to generate the required (optimized) cell voltage through a pre-arranged DC power supply units. Also, ECC eliminates shipping and handling of chemicals (example: liquid alum) which has been a challenge for small and remote communities located away from urban agglomerations [25]. Considering these many advantages of ECC, many researchers have carried out studies for treating different dye effluents [26], coffee effluents [27], health care effluents [28], grey wastewater [29], removal of organics from bilge water [30], for treating composite wastewater generating from industrial estates [31], strontium and cesium [32], removal of both arsenic and chromium from aqueous solution [33], chromium from water [34], phosphate removal from drinking water [35] and C.I. reactive blue dye removal [36]. Open literature shows little focus on (i) interdependence of operating parameters in treatment efficiencies and (ii) retaining water quality parameters after ECC and henceforth this research is proposed to overcome the research gaps.

In the present work, the laboratory scale investigations focus on finding out the optimum ECC operating conditions for arsenite removal from groundwater. Batch experiments were carried out to address the combined influence of the following: (i) number of electrodes immersed in the reactor for different cell voltages in a constant electrolyte volume, (ii) simultaneous changes in other bulk water quality parameters after ECC, (iii) electrode dissolution and sludge generation, (iv) energy consumption, and (v) operating cost.

2. Materials and methods

2.1. Chemicals and analytical methods

All the chemicals used in this research were of analytical reagent grade and was procured from Hi-Media Laboratories Pvt. Ltd., Mumbai, India. Physico-chemical water quality parameters were analyzed by the Standard Methods [37]. pH was measured using a pH meter (LI 127 Elico, India). The electrical conductivity of the solution was measured by a digital conductivity meter (Systronics Model 30/10FT YSI, India). Temperature variations in the bulk solution were recorded using a digital thermometer. Iron, nitrate, fluoride, sulfate and phosphate concentrations in the bulk solution were measured using a spectrophotometer. Arsenite in the form of arsenic and residual aluminum ion concentration in the solution was determined using inductively coupled plasma (ICP Horiba Jobin Yvon, France).

2.2. Characterization of groundwater

Groundwater was fetched from a local borewell source and analyzed for various drinking water parameters as per the Standard methods presented in Table 1. In the ECC

Table 1
Characterization of groundwater before ECC

Sl. No.	Parameter	Values	BIS (IS 10500-91, revised 2003) desirable limit
1	Temperature, °C	22–29	–
2	pH	7.52–7.73	6.5–8.5
3	Total alkalinity, (TA) as $CaCO_3$, mg/L	360–377	200
4	Electrical conductivity, (EC), μS/cm	807–1,075	300
5	Turbidity, NTU	0.29–1	5
6	Chloride, mg/L	70–91	250
7	Total hardness, (TH) as $CaCO_3$, mg/L	352–463	300
8	Calcium hardness, mg/L	140–160	75
9	Magnesium hardness, mg/L	212–253	30
10	Iron, mg/L	0.01–0.03	0.3
11	Sulfate, mg/L	34–46	200
12	Arsenic,mg/L	Nil	0.01
13	Total dissolved solids, mg/L	470–490	500

process, some of the water quality parameters favor in-situ coagulation–flocculation while some other parameters cause hindrance; the critical parameters that control the ECC treatment process are pH, alkalinity, and chlorides.

The background concentration of arsenic before ECC was 0 mg/L in the groundwater samples; henceforth, the groundwater samples before ECC were spiked with pre-estimated arsenite As(III) concentration of required value that factually prevail in arsenic prone ground water aquifers. For experimental purposes, a standard arsenite stock solution of 1,000 mg/L was prepared by dissolving a stoichiometric amount of sodium meta-arsenite ($NaAsO_2$), and the desired arsenite concentration was spiked to sampled groundwater to obtain the initial As(III) concentration. Arsenite was chosen because it is 25–60 times more toxic and mobile, predominantly found in arsenic affected groundwater and its removal is a challenge for environmental engineers and other water quality parameter values represent the actual groundwater composition of the sampling location which were well within the Indian BIS drinking water limits.

2.3. Experimental setup

The laboratory scale batch electrochemical coagulation process (BECC) unit was designed and fabricated using acrylic glass with effective volume of 2 L (170 mm × 120 mm × 110 mm) capacity. Iron plate electrodes of square shape (100 mm × 100 mm) with thickness of 1 mm placed at a pre-optimised electrode gap of 5 mm in parallel bipolar arrangement. The electrodes before and after were washed with 15% HCl solution before conducting each experiment to remove any dust. The difference in weight provides information on the anode dissolution useful in determining the operating cost. The current input to the electrochemical reactor (ECR) and the corresponding cell voltage was maintained constant using a precision DC power supply (Tektronix 35D (India), dual regulated power supply, 0–16 V, 0–10 A) unit. BECC was operated for applied cell voltages 6, 8, 12 and 16 V with uniform mixing in ECR, achieved using a magnetic stirrer (REMI 2MLH, India). All ECC test runs were performed at ambient temperature. In each run, 2 L of arsenite spiked groundwater of known initial concentration $As(III)_0$ was fed into the EC reactor. Experiments were carried out for the applied cell voltages with intent to observe the influencing parameters and changes in water quality during electrochemical treatment (ECT). Samples were retrieved at regular time intervals, filtered and analysed for residual arsenite concentration using ICP spectrometer (ICP Horiba JobinYvon, France) after each ECC run for a pre-determined electrolysis time (ET). After electrolysis, the electrodes were removed from ECR and the bulk solution was then allowed to stay quiescent for 5 min. A little while later, the supernatant was decanted, filtered and analysed for relevant physico-chemical water quality parameters. The solid residues (sludge) were collected in porcelain dishes and allowed for drying in a hot air oven at 102°C for further characterization.

3. Results and discussion

Arsenite removal in bipolar connection for different surface area/volume (SA/V) for different applied cell voltages during ECC is presented. Also, the changes in drinking water quality parameters after ECC are also presented.

3.1. Combined influence of applied cell voltages and SA/V ratio

The combined effect of the operating parameters such as increase in electrode numbers 4, 6 and 10, applied cell voltage 6 V, 8 V, 12 V and 16 V and SA/V: 40, 60 and 100 m^2/m^3 was investigated. The initial $As(III)_0$ concentration of 3.0 mg/L before ECC was maintained in all the ECC experiments to mimic ground reality. A series of BECC experiments were carried out to determine the overall effect of these influencing parameters on the arsenite removal process. Ali et al. [38] reported the chemical reaction involving the conversion of arsenite to arsenate in the ECC process as given in Eq. (1) and the produced arsenate was removed from water in a three-step process with oxidation of sacrificial anode, adsorption/replacement of the contaminants and settling of loosely aggregated mass of coagulant material along with arsenate.

$$AsO_2^- + 2OH^- \rightarrow H_2AsO_4^- + 2e^- \tag{1}$$

Figs. 1(a)–(d) show the arsenite degradation curves as a function of ET. In all the plots, a common removal trend was observed for all the applied cell voltages. With less number of electrodes (smaller SA/V), maximum arsenite removals were achieved. In other words, with an increase in the number of electrodes (larger SA/V), the arsenite removal efficiency reduced for all applied cell voltages. For an applied cell voltage of 6 V, the arsenite removal efficiency decreased with increase in electrode numbers for 4, 6 and 10 iron electrodes as presented in Fig. 1(a). At 45 min ET, arsenite concentration reduced to 0.03 mg/L for 4E (4 electrodes); 0.13 mg/L for 6E and 0.14 mg/L for 10E from its initial value. At an applied cell voltage of 8 V, the maximum reduction of arsenite concentration was 0 mg/L at 15 min for 4E and remained constant up to 60 min; 0.06 mg/L at 60 min for 6E and 0.11 mg/L at 60 min for 10E as shown in Fig. 1(b). At 12 V (SA/V: 40 m^2/m^3) a gradual decrease in arsenite removal was observed up to 15 min with As(III) of 0.06 mg/L and the arsenite was completely co-precipitated from the bulk solution between 15 and 45 min ET. Further treatment time up to 60 min was ascribed to the desorption process increasing the arsenite values to 0.18 mg/L (Fig. 1(c)). Using 6E, arsenite removal was observed up to 15 min, and later reappearance of the arsenite ion was observed (Table 4). Similarly, for 10E, As(III) concentration reached 0 mg/L at 60 min ET. It may be seen from the curves of Fig. 1(d), for 4E the arsenite removal was rapid and its concentration reached 0 mg/L within 10 min ET. For 6E and 10E, the concentration reached 0 mg/L within 15 min ET. For 16 V with an increase in electrode numbers, complete removal of arsenite was achieved within 10–15 min ET. There was no reappearance/desorption of arsenite ions into the bulk solution during the ECC treatment process; however, a premonition exists that if the ECC treated water is not passed through a filter sludge separation, the arsenite absorbed on the micro-sludge particles may re-entrain back into the treated water.

Considering the maximum arsenite removal rate in less treatment time, 16 V with 4E combination (SA/V: 40 m^2/m^3) proved effective and efficient. From the results, it was inferred that higher cell voltages provide higher current density for a fixed SA/V giving increased arsenite removal rates at short ETs.

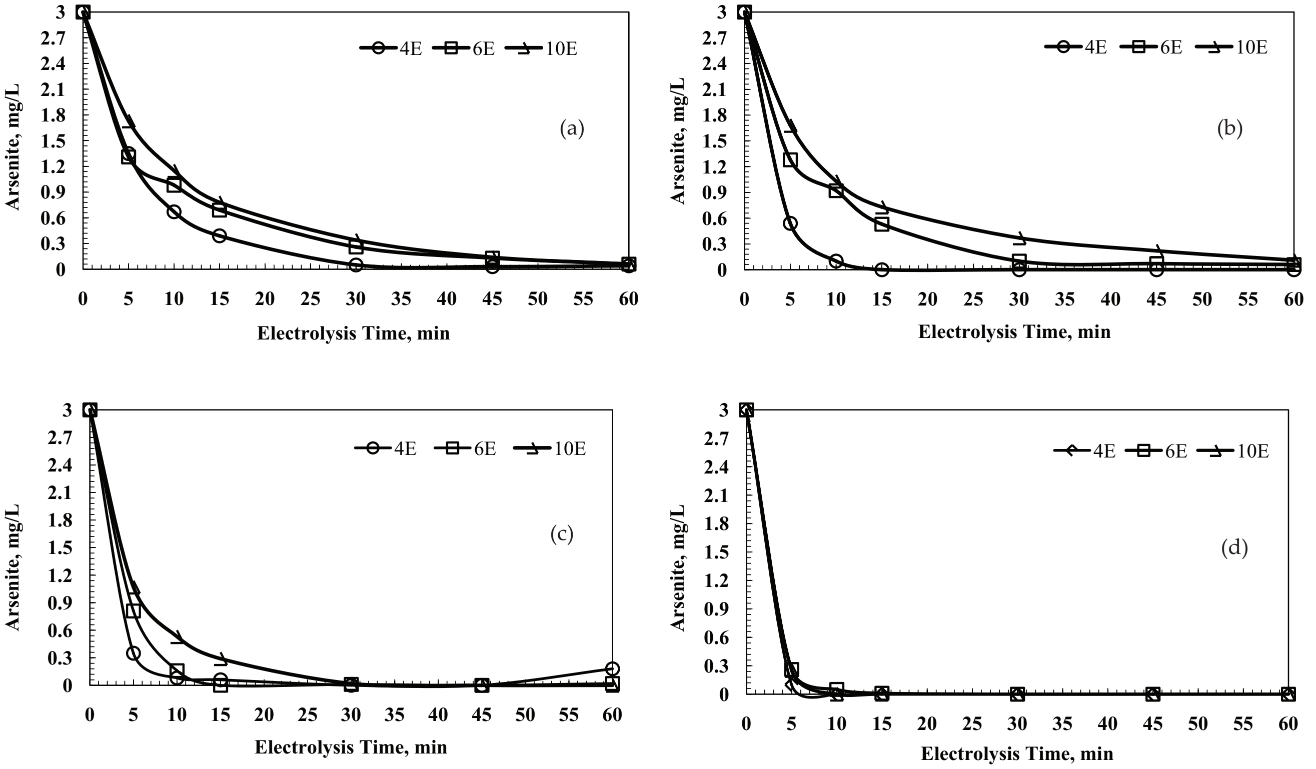

Fig. 1. Combined effect of electrode number (SA/V) and different applied cell voltages on arsenite concentration with ET for cell voltages (a) 6 V, (b) 8 V, (c) 12 V, and (d) 16 V. Operating conditions: $As(III)_0$: 3.0 mg/L; inter-electrode spacing: 5 mm; number of electrodes: 4; (SA/V of 40 m^2/m^3), 6 (SA/V of 60 m^2/m^3), and 10 (SA/V of 100 m^2/m^3), ET: 60 min.

Table 2
Variations in bulk solution characteristics during ECC for applied cell voltage of 6V for 4E, 6E, and 10E for $As(III)_0$ 3 mg/L

ET, min	6 V 4E				6 V 6E				6 V 10E			
	pH	EC, µS/cm	Color	As(III), mg/L	pH	EC, µS/cm	Color	As(III), mg/L	pH	EC, µS/cm	Color	As(III), mg/L
0	7.75	624	Colorless	3	7.65	528	Colorless	3	8.42	970	Colorless	3
5	7.73	616	Pale yellow	1.35	7.63	550	Colorless	1.31	8.26	969	Colorless	1.73
10	7.71	609	Yellow	0.67	7.67	597	Pale yellow	0.98	8.30	968	Pale yellow	1.15
15	8.0	591	Yellow	0.39	7.65	550	Pale yellow	0.69	8.32	964	Pale yellow	0.78
30	7.80	587	Rust brown	0.05	7.50	593	Yellow brown	0.26	8.17	961	Pale yellow	0.34
45	7.78	586	Bluish green	0.03	7.34	539	Dark rusty brown	0.13	8.14	948	Yellow	0.14
60	7.74	515	Dark green with blue tinge	0.04	7.34	530	Dark rusty brown	0.06	8.06	945	Yellow	0.06

3.2. Physico-chemical changes during the ECC process

ECC involves multiple complex reactions in a dynamic state during the hydraulic retention time. An observation on the combined effect of applied cell voltage (6–16 V) and SA/V is elaborated in Tables 2–5.

3.3. Bulk solution characteristics for 6 V

From Table 2 for an applied cell voltage of 6 V with electrode numbers 4E, 6E and 10E, the following observations were made.

3.3.1. Four iron electrodes with SA/V 40 m^2/m^3

The bulk solution color changed from colorless to pale yellow within 5 min ET because ferrous ions are oxidized to ferric ions by oxygen (Eqs. (2) and (3)) in the aqueous phase with a decrease in pH to 7.73 with a residual As(III) concentration of 1.35 mg/L.

$$Fe \rightarrow Fe^{2+} + 2e^{-} \tag{2}$$

$$Fe^{2+} + \frac{1}{4}O_2 + \frac{1}{2}H_2O \rightarrow Fe^{3+} + OH^{-} \tag{3}$$

The color of the solution retains its yellow color up to 15 min ET with solution pH value at 8 without any floc formation up to 30 min ET. At 30th min ET, brown color flocs formed when pH reached a value of 7.80 with residual As(III) concentration of 0.05 mg/L following the reaction in Eq. (4). The applied current forces the OH^- ion to migrate from cathode face to the anode face, so the pH near the anode is higher than in the bulk solution; such a situation favors the formation of ferric hydroxide which appears as a red-brown colloid [39]; while treating 4-nitrophenol from aqueous solution by electrocoagulation states that formation of a gelatinous precipitate made of $Fe(OH)_3$ hydrous oxide occurs for pH > 4.

$$Fe^{3+} + OH^- \rightarrow Fe(OH)_3 \downarrow \quad (4)$$

From 45–60 min ET, the solution color turned to dark bluish green at pH 7.74–7.78 with residual As(III) concentration of 0.03–0.04 mg/L following Eq. (5). This dark bluish green color is because of the formation of $Fe(OH)_2$ (Eq. (5)). Based on the pH of the medium, the color keeps changing from yellow → green → blue from acidic pH to basic pH. Flocs generated in the ECR showed green color mainly because of the formation of ferrous oxide [40].

$$Fe^{2+} + OH^- \rightarrow Fe(OH)_2 \downarrow \quad (5)$$

3.3.2. Six iron electrodes with SA/V 60 m^2/m^3

Using six iron electrodes for the same cell voltage of 6 V, the bulk solution color changes from colorless to pale yellow after 10 min (double the time for 4E) of ET. The applied cell voltage of 6 V was not sufficient enough for electrode dissolution as the voltage/current gets distributed over a large area. Pale yellow color indicates the liberation of Fe^{3+} ions into the solution. As the solution turns brown at ~45 min ET, the floc appear at pH 7.34–7.50 to form a floc matrix for entrapment of As(III).

3.3.3. Ten iron electrodes with SA/V 100 m^2/m^3

In this case, pale yellow color of the solution remains as is because of the Fe^{3+} formation as reported by Sadeddin et al. [41] up to 45 min without floc formation. After 45 min ET, the solution turns dark yellow with the micro-floc formation with As(III) concentration reduced to 0.06 mg/L at pH 8.06–8.14. Finally, for applied cell voltage of 6 V maximum arsenite is reduced to 0.03 mg/L for 4E (SA/V 40 m^2/m^3).

3.4. Bulk solution characteristics for 8 V

Table 3 shows the changes observed during the ECC process while using 8 V for an HRT of 60 min using four iron electrodes (4E) in a bipolar mode. The color of the bulk solution changed from colorless → yellow brown → brownish yellow → dark green → light bluish green → light greenish blue in sequence with a marginal decrease in pH from 8.14 to 8.12. The As(III) concentration in the bulk solution reached 0 mg/L within 15 min ET; explaining the fact that a larger cell voltage spread over a small area (40 m^2/m^3) which provides quicker removal of As(III).

Similarly, for 6E by 30 min ET, the solution color changed from pale yellow to brown with As(III) concentration reaching 0.10 mg/L. The formation of $Fe(OH)_2$ floc produces a green color displaying its state of maturity and stability at which the As(III) concentrations in the bulk solution reached 0.06–0.07 mg/L at 60 min ET.

For an SA/V of 100 m^2/m^3 (10E), ECC does not manifest assisting removal. The pale yellow color remains unchanged showing the presence of Fe^{3+} ions in large quantities without enough charge strength to neutralize the colloids. Also, the applied cell voltage was not sufficient enough to carry out ECC reactions up to 45 min. At the end of 60 min ET, the bulk solution turns yellowish brown with pH 7.90 having residual arsenite concentration of 0.11 mg/L. Table 3 shows, with four iron electrodes within 15 min of ET the As(III) concentration was reduced to 0 mg/L indicating that, lesser the number of electrodes, the removal efficiency is more within a short ET.

3.5. Bulk solution characteristics for 12 V

The change in bulk solution characteristics is shown in Table 4 for 4E, 6E, and 10E using 12 V. The color changing sequence is from colorless → yellow → green → bluish dark green → pale bluish green → pale blue → whitish pale blue

Table 3
Variations in bulk solution characteristics during ECC for applied cell voltage of 8 V for 4E, 6E and 10E for $As(III)_0$ 3 mg/L

ET, min	8 V 4E				8 V 6E				8 V 10E			
	pH	EC, µS/cm	Color	As(III), mg/L	pH	EC, µS/cm	Color	As(III), mg/L	pH	EC, µS/cm	Color	As(III), mg/L
0	8.14	632	Colorless	3	7.42	625	Colorless	3	8.15	987	Colorless	3
5	8.23	638	Yellow brown	0.54	7.30	636	Pale yellow	1.28	8.02	988	Pale yellow	1.68
10	8.02	640	Brownish yellow	0.10	7.33	623	Pale yellow	0.92	7.97	982	Pale yellow	1.03
15	7.98	630	Brownish yellow	0.0	7.38	635	Rust brown	0.53	7.99	989	Pale yellow	0.73
30	7.91	603	Dark green	0.0	7.53	610	Dark brown	0.10	7.94	970	Pale yellow	0.37
45	8.01	541	Light bluish green	0.0	7.64	591	Greenish yellow	0.07	7.87	961	Pale yellow	0.22
60	8.12	524	Light greenish blue color	0.0	7.56	596	Pale green	0.06	7.90	951	Yellowish brown	0.11

for 4E with pH varying from 7.81 to 9.33, with a decrease in As(III) concentration from 3 to 0.18 mg/L at 60 min ET.

Similarly, for 6E the color change sequence was: colorless → pale yellow → brown → dark green → dark green with white tinge → whitish green at 60 min ET. As(III) values reduced to 0 mg/L at 15 min with pH$_f$ 7.53. Once the contaminants were removed, desorption commenced after 30 min with As(III) re-entraining into the solution (0.01 mg/L). Pale yellow color persisted upto 30 min with 10E with residual As(III) concentration of 0.29 mg/L in the solution. Formation of brown and green colored floc was observed at ~50 min with pH values of 7.43 and As(III) values reaching zero at 60 min ET.

3.6. Bulk solution characteristics for 16 V

Table 5 shows the changes in 16 V for color, conductivity, and arsenite values while using (electrode numbers of 4E, 6E, and 10E, SA/V: 40, 60, and 100 m^2/m^3). However, color changes were observed from colorless → yellow → green → greenish white → grey. The formation of $FeCl_2$ and $FeCl_3$ gives greenish white color. The bulk solution slowly turns from grey to black indicating the formation of black anhydrous magnetite (Fe_3O_4).

The electrochemical reaction rate increases when the temperature of the solution increases. It was observed that as the temperature of the solution increases, the arsenite removal efficiency improves marginally reasons ascribed to increase in mobility and collision of ions with the polymeric hydroxides. The pH change in the bulk solution was 2 units (pH$_0$: 7.4 and pH$_f$: 9.37) for SA/V of 40 m^2/m^3 (4E) and lower by one unit for SA/V: 40 m^2/m^3 (10E). The increase in pH in all the cases is also attributed to the formation of ferric hydroxide species together with the attack on the cathode by the hydroxyl ions which lead to a very small increase in pH as stated by Mahesh et al. [42] with the increase in SA/V. Reduction in conductivity values were more significant at 4E compared with 6E and 10E configurations. A decrease in pH occurred during the ECC process with a simultaneous increase in the current across the electrodes.

The pathway of changes in color while using six iron electrodes is shown in Table 5. The color change that occurred in the sequence was: colorless → pale yellow → green →

Table 4
Variation in bulk solution characteristics during ECC for applied cell voltage of 12 V for 4E, 6E and 10E for As(III)$_0$ 3 mg/L

ET, min	12 V 4E				12 V 6E				12 V 10E			
	pH	EC, µS/cm	Color path	As(III), mg/L	pH	EC, µS/cm	Color path	As(III), mg/L	pH	EC, µS/cm	Color path	As(III), mg/L
0	7.81	640	Colorless	3	7.63	594	Colorless	3	7.47	998	Colorless	3
5	7.66	644	Rust yellow	0.35	7.56	610	Pale yellow	0.81	7.40	992	Pale yellow	1.07
10	7.82	645	Green	0.08	7.41	606	brown	0.16	7.41	994	Pale yellow	0.53
15	7.86	629	Bluish dark green	0.06	7.53	607	Dark green	0	7.42	985	Pale yellow	0.29
30	8.45	641	Pale bluish green	0	7.68	585	Dark green	0.01	7.41	971	Yellow brown	0.02
45	8.87	584	Pale blue	0	7.17	518	Dark green with white tinge	0	7.47	965	Green	0
60	9.33	566	White with pale blue	0.18	7.96	480	Whitish green	0.02	7.52	939	Green	0

Table 5
Variations in bulk solution characteristics during ECC for 16 V for 4E, 6E, and 10E for As(III)$_0$ 3 mg/L

ET, min	16 V 4E				16 V 6E				16 V 10E			
	pH	EC, µS/cm	Color path	As(III), mg/L	pH	EC, µS/cm	Color path	As(III), mg/L	pH	EC, µS/cm	Color Path	As(III), mg/L
0	7.4	664	Colorless	3	7.62	644	Colorless	3	7.48	1,004	Colorless	3.0
5	7.45	650	Yellow	0.10	7.49	628	Pale yellow	0.26	7.46	1,002	Pale yellow	0.25
10	7.72	650	Green	0	7.66	623	Green	0.05	7.51	993	Greenish brown	0
15	8.13	622	Dark green	0	7.71	596	Dark green	0.01	7.73	999	Brownish green	0
30	8.75	592	Greenish white	0	7.61	513	Pale bluish green	0	7.80	966	Pale bluish white	0
45	9.50	442	Grey	0	7.95	474	Pale bluish green	0	7.90	908	Pale bluish white	0
60	9.37	495	Grey	0	8.53	461	Pale bluish green	0	7.89	871	Pale bluish white	0

pale bluish green because of the formation of sulfides of iron oxides. When using 10 iron electrodes, color changing sequence of the bulk solution was: colorless → pale yellow → greenish brown → brownish green → pale bluish white at 60 min ET. This change in bulk solution color is due to the formation of Fe^{3+}, oxides of $Fe(OH)_2$, oxides of $Fe(OH)_3$, oxides of sulfates, phosphates, chlorides results in pale bluish white in color. Also, this micro-change in pH is because of other mechanisms such as over saturation of CO_2 in the acidic aqueous phase. First, the electrolyte tend to release from the medium owing to a disturbance in the hydrogen bubbles which increase the pH value, and second, because of some anions such as Cl^- and SO_4^{2-} present in water which exchange partly with OH^- to free OH^- resulting in the increase of the bulk solution pH.

Summarizing, it was interpreted that the operating parameters: applied cell voltage, cell volume, electrolyte quality and quantity, electrode numbers, SA/V, pH, and the chemical composition of the medium – all of these are interlinked and inter-dependent on each other and play their discrete role in the ECC process. Keen observations in the color changes of the bulk solution showed that maximum arsenite removals could be achieved when the floating scum atop the ECR appears green marking the maturation state of the ECC process. The highest cell voltage of 16 V resulted in maximum arsenite removal at a very short HRT of 45 min. Thus, maximum arsenite removal from its initial concentration of 3 to 0 mg/L was achieved for the optimal operating condition having inter-electrode spacing: 5 mm; number of electrodes: 4 (SA/V of 40 m^2/m^3); applied cell voltage of 16 V and 45 min of ET proved effective.

4. Changes in drinking water quality parameters after ECT

After undergoing several complex reactions in the electrochemical reactor, the water quality characteristics change with time as the treatment progresses. During each ECC, the co-occurring solutes present in groundwater undergo various chemical reactions in the presence of M^+ ions resulting in both redox and displacement reactions. The charged M^+ ions in the solution during treatment pick up micro-flocs from the solution which participates in the sweeping mechanism along with it the target contaminants from the solution finally reaching the top of the ECR as floating gel. The gel matrix contains micro-bubbles of $H_{2(g)}$, $O_{2(g)}$, and $Cl_{2(g)}$, etc., which are released from the electrodes showing the evidence of chemical reactions occurring in the ECC process. In order to measure the changes from its wholesomeness, various water quality parameters such as pH, temperature, conductivity, alkalinity, total hardness, calcium, magnesium, chloride, sulfate, chloride/sulfate ratio, iron, nitrate, phosphate, arsenic, and aluminium were analysed after ECC as per the APHA [37] standard methods. The concentrations of various drinking parameters representing water quality after 60 min ET are shown in Table 6.

From Table 6 it may be observed that after ECC treatment, for the applied cell voltage of 6 V and SA/V ratios of 40, 60, and 100 m^2/m^3, at 60 min ET the corresponding pH values were 7.74, 7.34, and 8.06, slightly reduced from its original value of 7.75, 7.65, and 8.42. Similarly, reduction in pH for 60 m^2/m^3 to 8.12, 7.56, and 7.90 from initial values of 8.14, 7.42, and 8.15 for 8 V with SA/V ratio of 40, 60, and 100 m^2/m^3 was observed, respectively. The decrease in pH value during the ECC process is because of formation of H^+ ions due to Cl_2 reaction in water as per the equations given by [43,44] and also during the formation of iron hydroxides, H^+ ions is liberated which lowers the solution pH as also reported by Arienzo et al. [45] and also during ClO_2 formation as explained by Eqs. (6)–(9).

$$Cl_2 + H_2O \rightarrow HOCl + H^+ + Cl^- \tag{6}$$

$$HOCl \rightarrow H^+ + OCl^- \tag{7}$$

Table 6
Post ECC drinking water quality characteristics

Water quality parameters	Raw groundwater	Specific area to volume (SA/V), m^2/m^3											
		40, m^2/m^3				60, m^2/m^3				100, m^2/m^3			
		6 V	8 V	12 V	16 V	6 V	8 V	12 V	16 V	6 V	8 V	12 V	16 V
pH	7.52–7.73	7.74	8.23	9.33	9.37	7.54	7.56	7.69	8.53	8.06	7.9	7.67	7.89
Temperature, ◦C	22–29	25.8	25	27.2	25.8	25	26.90	26	27.9	22	21.1	21.8	25
Conductivity, µS/cm	807–1,075	515	524	566	495	530	596	480	461	945	951	933	871
Turbidity, NTU	0.20–1	5.2	5.4	4.1	3.6	4.10	3	0.0	1.70	5.7	3.6	5.2	3
Total alkalinity as $CaCO_3$, mg/L	360–377	276	276	172	136	196	308	248	172	349	348	340	228
Total hardness as $CaCO_3$, mg/L	352–463	272	268	200	176.0	292	260	224	180	432	328	304	240
Calcium, mg/L	140–160	76	72	88	72	104	88	76	56	120	164	108	80
Magnesium, mg/L	212–253	196	196	112	104	188.0	172	148	124	312	164	196	160
Chloride, mg/L	70–91	56.7	56.7	74.36	78.27	66.53	70.45	58.7	82.19	90	72.4	91.54	91.97
Sulfate, mg/L	34–46	34.91	29.30	40.44	25.6	95.58	51.79	21.43	33.72	43.04	17.92	69.5	40.67
Iron, mg/L	0.01–0.03	0.13	1.41	0.07	0.11	4.90	3.32	0.6	0.13	0.68	0.2	0.19	0.83
Arsenic, mg/L	3. 0	0.04	0	0.18	0	0.06	0.06	0.02	0	0.06	0.11	0	0

$$\mathrm{Cl^- + H_2O \rightarrow ClO_2 + 4H^+ + 5e^-} \tag{8}$$

$$\mathrm{Fe(III) + 3H_2O \rightarrow Fe(OH)_3 + H^+} \tag{9}$$

The Cl^- ions in solution also get oxidized at the anode directly to ClO_2 Eq. (10):

$$\mathrm{Cl^- + 2H_2O \rightarrow ClO_2 + 4H^+ + 5e^-} \tag{10}$$

As the applied cell voltage increased to 12 and 16 V for 40, 60, and 100 m^2/m^3, pH_f marginally increased from its pH_0. The reason for the increase in pH is primarily because of ferrous ions Fe^{2+} released from the active face of the iron electrodes. When the applied cell voltage exceeds a certain value, hydrogen evolution begins and as a result, pH of the water increases with an increase in the concentration of the hydroxyl ions as shown by the reaction in Eq. (11).

$$\mathrm{2H_2O + 2e^- \rightarrow H_2 \uparrow + 2OH^-} \tag{11}$$

Ching et al. [46] reported that, although coagulation with iron salts occurs on a wide pH range through various mechanisms, amorphous ferric hydroxide is least soluble at bulk solution pH value of ~8. The precipitation of ferric hydroxide at elevated pH gives rise to sweep flocculation mechanism as an end step. Therefore, increase in bulk solution pH in an ECR because of hydrogen evolution becomes an advantageous situation from the viewpoint of coagulation. Because of the occurrence of various exothermic chemical reactions during the ECC process, a gradual increase in the bulk solution temperature occurs after the ECC process.

The decrease in conductivity values for different SA/V ratios and applied cell voltages indicates ion pairing or multiple-ion association between solvated species and opposite charges and simultaneous anions and cations precipitated out of the solution [47]. The turbidity of the bulk solution after ECC increased because of the presence of hydroxide iron flocs which was later entirely removed by simple filtration using carbon as a medium. Hardness causing salts were also removed after the desired ET for all cell voltages and SA/Vs. This is because of a high pH in the vicinity of the cathode face and forced precipitation of carbonate salts on the electrodes. This statement is justified by the increase in the electrode weight after electrolysis because of deposits caused by the carbonate salts. The hardness removal mechanism is shown in Eqs. (12)–(14).

$$\mathrm{Ca^{2+} + OH^- \rightarrow Ca(OH)_2 \downarrow} \tag{12}$$

$$\mathrm{Mg^{2+} + OH^- \rightarrow Mg(OH)_2 \downarrow} \tag{13}$$

$$\mathrm{Mg^{2+} + CO_3^{2-} \rightarrow MgCO_3 \downarrow} \tag{14}$$

The added benefit of the formation of $Mg(OH)_2$ and $Ca(OH)_2$ flocs is that, it facilitates entrapment and enmeshment of As(III) into the gel-like floc matrix as precipitates which removes As(III), magnesium, and calcium ions. The reduction in calcium and magnesium concentrations is explained by the precipitation of carbonate and sulfate salts near the cathode face at pH > 8 resulting from the reaction in the cathodic zone as shown in Eq. (15).

$$\mathrm{H_2O + 2e^- \rightarrow H_2 + 2OH^-} \tag{15}$$

The most crucial bulk water properties that mainly influence the ECC process in our work are total alkalinity, temperature, and chlorides. Alkalinity reduction after ECC occurs because of the evolution of gaseous CO_2 increasing the pH of the bulk solution from its influent pH; because alkalinity gets consumed thereby facilitating the optimum coagulating pH producing effective coagulation. The calcium bi-carbonate ($3Ca(HCO_3)_2^-$), bicarbonate ($3HCO_3^-$), and carbonate ions CO_3^{2-} present in the bulk solution reacts with ferrous ions forming $Fe(OH)_3$ resulting in alkalinity consumption as shown by the reactions in Eqs. (16)–(18).

$$\mathrm{Fe^{3+} + 3HCO_3^- \rightarrow Fe(OH)_3 \downarrow + CO_2 \uparrow} \tag{16}$$

$$\mathrm{Fe^{3+} + CO_3^{2-} + 3H_2O \rightarrow 2Fe(OH)_3 \downarrow + CO_2 \uparrow} \tag{17}$$

$$\mathrm{Fe^{3+} + SO_4^{2-} + 3Ca(HCO_3)_2^- \rightarrow 2Fe(OH)_3 + 3CaSO_4 + 6CO_2 \uparrow} \tag{18}$$

The sulfate ions are also reduced because of the precipitation of calcium sulfate as $CaSO_4$ following Eq. (18). The exothermic reactions during ECC increase the water temperature by 1°C–2°C which marginally improves the treatment efficiency. Further, chloride concentration in the bulk solution after EC treatment also reduced by 21.75% and 18.28% for SA/V of 40 and 60 m^2/m^3, respectively. Similarly, for SA/V of 100 m^2/m^3 for 12 and 16 V, the average chloride concentration increased by 7.69% and 8.2%, respectively. For an SA/V of 40 m^2/m^3 as the cell voltage increases from 6 to 16 V, the chloride concentration after 60 min ET also increased to 56.7, 56.7, 74.36, and 78.27 mg/L. Similarly, for SA/V 60 m^2/m^3 for an increase in cell voltage, the chloride concentrations were 66.53, 70.45, 58.7, and 82.19 mg/L, respectively. Further, for SA/V 100 m^2/m^3, the chloride concentrations were 90, 72.4, 91, and 91 mg/L. The pattern of Cl^- values can be logically explained by the electrochemical discharge of chlorine at the anode face (as a secondary electrochemical reaction) at pH < 2 as $Cl_{2(g)}$ according to the Pourbiax diagram of chlorine is represented by Eq. (19).

Since all the ECC experiments were carried out for natural drinking water pH, the effect of low pH does not arise and so only hypochlorous acid (HOCl) and hypochlorite ion (OCl^-) species were released enhancing the rate of the electrochemical reactions by inducing pitting corrosion. The presence of chloride salts in water in relatively high concentrations assists in the production of chlorine by Eq. (18), which increase the erosion on the anode face. The cathode face also partially erodes because of the bombardment of charged M^+ ions. Chlorine behaves similar to an oxidizing agent which participates in oxidizing soluble ferrous ions into insoluble ferric ions [48]. Kraft [49] reports that chloride values at concentrations <100 mg/L is sufficient to produce free chlorine to efficiently disinfect water.

$$2Cl^- \rightarrow Cl_2 + 2e^- \tag{19}$$

This chlorine hydrolyzes in water and forms HOCl as shown by the reaction in Eq. (20):

$$Cl_2 + H_2O \rightarrow HOCl + H^+ + Cl^- \tag{20}$$

The HOCl and the OCl^- form a pH-dependent equilibrium as follows:

$$HOCl \rightarrow OCl^- + H^+ \tag{21}$$

The sum of HOCl and OCl^- is referred as free chlorine or active chlorine. Its disinfecting effect is based on the release of atomic oxygen according to Eqs. (22) and (23) as follows:

$$HOCl \rightarrow O + Cl^- + H^+ \tag{22}$$

$$OCl^- \rightarrow O + Cl^- \tag{23}$$

During the electrochemical disinfection process, chloride ions which were consumed by electrochemical reactions for free chlorine production are again reformed. The overall effect is that there is no change in the chemical composition of the water after electrochemical disinfection. The chloride value also increases the electrical conductivity of the solution which inhibits the formation of a passive layer on the faces of the electrodes (anode). In general, the chloride ions present in water undergo various reactions and the chloride ions so generated is consumed in multiple electrochemical reactions with an end effect of a decrease in the chloride concentrations of the bulk solution after ECC. Contrastingly, for SA/V 100 m^2/m^3 there was no reduction in chloride values implying that oxidation of organics depends mostly on the active chlorine generated during electrolysis. For increased SA/Vs, the applied cell voltage becomes meager for further secondary chemical reactions to follow and manifest to reach the maturation phase in the ECR.

In any drinking water ECC process using iron salts or iron balls/plates/sheets as electrodes, the residual metal ion concentration in the treated water is of prime importance. For complete ECC treatment, either a longer ET is required applying medium cell voltages, or a larger cell voltage is needed or both depending on the chosen SA/V value. From Table 6, it may be observed that the residual iron concentration determined using atomic absorption spectroscopy in the treated water was found to be well within the BIS 10500 (1993 & 2003) [50] limits of 0.3 mg/L for cell voltages viz., 6–16 V 4E, 12–16 V 6E, and 16 V 10E showing a complete oxidation process. In rare cases, when using lower applied cell voltages (6–12 V), iron concentration in water sometimes exceed 0.3 mg/L indicating partial and incomplete oxidation/ECC process for 100 m^2/m^3 SA/V (10E).

It was concluded from the present research experience that if one intends to lower the HRT for a quick treatment, large number of electrodes (higher SA/V) are required and a corresponding larger cell voltage to get the positive effect of not allowing release of metal ions into solution. Further, all other cations and anions present in water such as nitrate and phosphates after treatment were found to be well within the Bureau of Indian Standards (BIS-10500) for drinking water quality standards for all the applied cell voltages and all SA/Vs.

Summarizing the pre and post ECC water quality characteristics, it was concluded that for applied cell voltages ranging from 6 to 12 V for 40, 60 and 100 m^2/m^3 SA/V, a marginal increase in total alkalinity and residual iron concentration with unsatisfactory As(III) removals were observed. However, when using cell voltage of 16 V with SA/V ratio of 40 m^2/m^3, the water quality parameters were kept well under quality control; this operating condition was considered as the best operating condition for ~100% As(III) removal.

5. Electrode dissolution and ECC sludge generation

The active coagulant (M^+) ion generated by electro-dissolution reacts with OH^- ions to form hydroxides. These hydroxides entrap contaminants, and the micro bubbles assist in adsorption and precipitation which float atop the reactor. These micro-precipitates further agglomerate slowly to form a jel-like sludge. The amount of metal dissolution and the sludge generated during the ECC process is shown in Figs. 2(a) and (b) for different SA/V and applied cell voltages. From the plot, it may be observed that at a particular cell

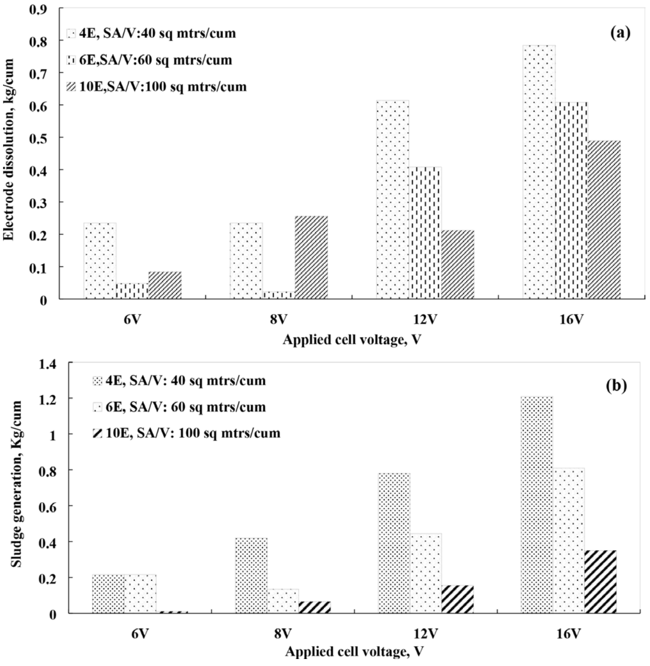

Fig. 2. Combined effect of cell voltage, electrode number and SA/V. (a) ED as a function of applied cell voltage for different SA/V and (b) sludge generation as a function of applied cell voltage for different SA/V.

voltage for increasing SA/V, the electrode dissolution (ED) decreases. For 16 V, the ED showed a decreasing trend from 0.7838, 0.607, and 0.489 kg/m^3 with increase in the electrode numbers 4, 6, and 10E.

Fig. 2(b) shows the amount of dried sludge generated for different cell voltage at different SA/V's. The histogram plot shows a decrease in sludge production with the increase in the number of electrodes for the same applied cell voltage. On the other hand, the quantity of sludge generated increases with the increase in cell voltage for a particular SA/V. The maximum ED of 0.7838 kg/m^3 with a corresponding dry sludge generation of 1.21 kg/m^{3}was obtained for 16 V 4E at 60 min ET. Therefore, it was observed that with an increase in cell voltage at lower SA/Vs, ED increases with an increase in sludge volume for a fixed electrolyte volume.

6. Energy consumption, operating cost, and electrode passivation

A significant issue associated while applying ECC as a better treatment option is its energy consumption, operating cost and electrode passivation. All these parameters assist in determining the feasibility of the treatment. From the above results obtained, it was found that the optimal operating condition concerning arsenite removal was 16 V with 4E iron electrodes (40 m^2/m^3) with a short HRT of 60 min. The energy consumption and operating cost were determined using Eq. (24) as follows:

$$\text{Operating cost} = aC_{\text{energy}} + bC_{\text{electrode}} + cC_{\text{chemical}} \tag{24}$$

where, C_{energy} is the energy consumption in kWh per m^3 of treated water estimated using Eq. (25).

$$C_{\text{energy}} = \frac{VIt}{\text{Treated volume}(l)} \tag{25}$$

$C_{\text{electrode}}$ is the electrode consumption in kg per m^{3}of water treated, estimated using Eq. (26).

$$C_{\text{electrode}} = \frac{ItM_w}{ZFV} \tag{26}$$

where I is the current (A), t is the ET in seconds, M is the molecular mass of iron (0.05585 kg/mol) and aluminum (0.02968 k/mol), Z is the number of electrons transferred for iron (Z_{Fe} = 2) and aluminum (Z_{Al} = 3), F is the Faraday's constant (96,485 C/mol), and V is the volume of effluent treated (in Eqs. (25) and (26)) in m^3. $C_{\text{chemicals}}$ is the chemical consumption in kg per m^3 of water treated. Unit prices, a and b are as follows: *a* is the electrical energy prices of (INR) Rs. 2.90 per unit for rural areas within 30 units power consumption as per the Karnataka tariff 2016; *b* is electrode material price is 50 INR per kg of iron sheets. On bulk purchase, *c* is the price of chemicals which is zero INR/kg, as no chemicals are used as additives/aid in the treatment process.

Fig. 3 shows the effect of SA/V on energy consumption, operating cost and passivation factor while using iron plate electrodes in a bipolar arrangement for 4, 6, and 10 electrodes (40, 60, and 100 m^2/m^3) SA/V. From Fig. 3, it may be observed that maximum energy consumption was found at 12 V with 4E and 6E followed by 16 V 6E with energy consumption varying from 0.68 to 1.69 kWh/m^3.

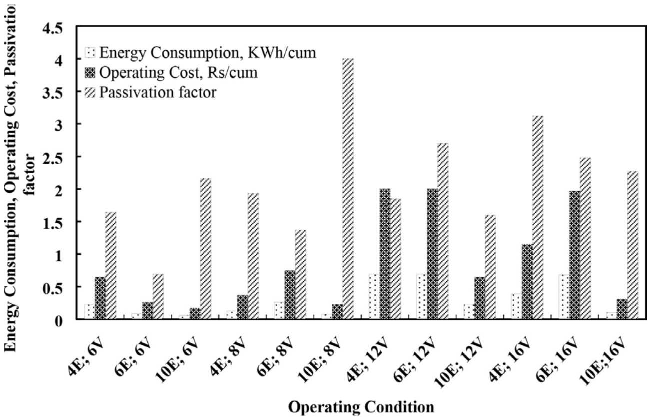

Fig. 3. Combined effect of applied cell voltage, number of electrodes and SA/V ratio on: energy consumption, passivation factor, and operating cost after 60 min ET.

The operating cost is the sum of energy consumption cost, electrode cost, and chemical cost. Eq. (24) shows that operating cost is directly proportional to all the above three components; for 16 V the operating cost was Rs. 1.15, 1.97, and 0.31/m^3. Overall, it was observed that increasing the current density of fixed water volume causes a proportional increase in the ohmic voltage losses, which indirectly increases the energy consumption. Comparison of arsenic decontamination efficiencies of chemical coagulation and EC is reported by Nidheesh and Singh [51] and thus based on the ECC treatment proved to be more efficient than other treatment process.

7. Conclusions

The present study demonstrates that ECC with the optimal operating conditions can be employed as a useful treatment option for arsenite removal from groundwater using iron electrodes in a bipolar mode. The following conclusions are drawn:

- Applied cell voltage and SA/V are inter-dependent for ECRs operating on a fixed volume which is an important parameter that influences the production of in-situ coagulant ions. Low cell voltages with increase in electrode number resulted in a small sized flocs reducing the arsenite removal efficiency.
- All the drinking water quality parameters after ECC treatment were well within the desired BIS standards, and WHO for optimal 16 V, 4E electrode combinations.
- The electrode dissolution and amount of sludge generated are directly proportional to the applied cell voltage and inversely proportional to the electrode numbers. The prime focus was on arsenite removal efficiency, loss of electrode material, sludge control, passivation, water quality, energy consumption, and operating cost. The operating conditions viz., inter-electrode spacing: 5 mm, no. of electrodes: 4, applied cell voltage: 16 V, SA/V ratio: 40 m^2/m^3 and ET: 45 min proved to be an effective

operating condition for treating $As(III)_0$ values ranging from 1 to 3 mg/L. Also, for this operating condition the beneficial mineral content of water was restored without imparting secondary contaminants into the treated water. The energy consumption and operating cost for the applied cell voltage of 16 V with 4 iron electrodes is 0.397 KWh/m^3 and Rs.1.15 per every cubic meter of water treated. Hence, ECC is a novel treatment technology which proves both effective and efficient in removing arsenite from groundwater with a small filtration unit downline the ECC unit.

References

[1] E. Lacasa, P. Canizares, C. Saez, F.J. Fernandez, M.A. Rodrigo, Removal of arsenic by iron and aluminium electrochemically assisted coagulation, Sep. Purif. Technol., 79 (2011) 15–19.

[2] S.L. Wang, C.H. Liu, M.K. Wang, Y.H. Chuang, P.N. Chiang, Arsenate adsorption by Mg/Al-NO_3 layered double hydroxides with varying the Mg/Al ratio, Appl. Clay Sci., 43 (2009) 79–85.

[3] V.K. Gupta, I. Ali, Environmental Water: Advances in Treatment, Remediation and Recycling, Elsevier, The Netherlands, 2012.

[4] C. Swapnila, S.J.S. Flora, Arsenic and fluoride: two major groundwater pollutants, Indian J. Environ. Biol., 48 (2010) 666–678.

[5] B. Petrusevski, S. Sharma, J.C. Schippers, K. Shordt, Arsenic in Drinking Water – Thematic Overview Paper Vol. 17, IRC International Water and Sanitation Centre, 2007, pp. 8–9.

[6] A. Mukherjee, M.K. Sengupta, M.A. Hossain, S.Ahamed, B. Das, B. Nayak, D. Lodh, M.M Rahman, D. Chakraborti, Arsenic contamination in groundwater: a global perspective with emphasis on the asian scenario- review article, J. Health Popul. Nutr., 24 (2006) 142–163.

[7] N.E. Korte, Q.A. Fernando, Review of arsenic (III) in groundwater, Crit. Rev. Environ. Control., 21 (1991) 1–39.

[8] T.S.Y. Choong, T.G. Chuah, Y. Robiah, F.L.G. Koay, I.Azni, Arsenic toxicity, health hazards and removal techniques from water: an overview, Desalination, 217 (2007) 139–166.

[9] I. Ali, T.B. Khan, M. Asim, Removal of arsenic from water by electrocoagulation and electrodialysis techniques, Sep. Purif. Rev., 40 (2011) 25–42.

[10] I. Ali, T.A. Khan, H. Iqbal, Treatment and remediation methods for arsenic removal from the ground water, Int. J. Environ. Eng., 3 (2011) 48–71.

[11] I. Ali, Z.A. Al-Othman, A.R. Alwarthan, M. Asim, T.A. Khan, Removal of arsenic species from water by batch and column operations on bagasse fly ash, Environ. Sci. Pollut. Res., 21 (2014) 3218–3229.

[12] I. Ali, H.Y. Aboul-Enein, Speciation of arsenic and chromium metal ions by reversed phase high performance liquid chromatography, Chemosphere, 48 (2002) 275–278.

[13] I Ali, C.K. Jain, Advances in arsenic speciation techniques, Int. J. Environ. Anal. Chem., 84 (2004) 947–964.

[14] B. Ghosh, M.C. Das, A.K. Gangapadhyay, T.B. Das, K. Singh, S. Lal, S. Mitra, S.H. Ansari, T.K. Goswami, S.K. Chakraborty N.N. Banerjee, Removal of arsenic from water by coagulation treatment using iron and magnesium salt, Indian J. Chem. Technol., 10 (2003) 87–95.

[15] S.K. Tiwari, V.K. Pandey, Removal of arsenic from drinking water by precipitation and adsorption or cementation: An environmental prospective, Recent Res. Sci. Technol., 5 (2013) 88–91.

[16] M.A. Jalil, F. Ahmed, Development of An Activated Alumina Based Household Arsenic Removal Unit, pp. 131–145.

[17] R. Ansari, M. Sadegh, Application of activated carbon for removal of arsenic ions from aqueous solutions, E-J. Chemistry, 4 (2007) 103–108.

[18] M. Barakat, S.I. Shah, Utilization of anion exchange resin spectra/gel for separation of arsenic from water, Arab. J. Chem., 6 (2013) 307–311.

[19] I. Ali, Microwave assisted economic synthesis of multi walled carbon nanotubes for arsenic species removal in water: batch and column operations, J. Mol. Liq., 263 (2018) 442–453.

[20] I. Ali, V.K. Gupta, T.A. Khan, M. Asim, Removal of arsenate from aqueous solution by electrocoagulation method using Al-Fe electrodes. Int. J. Electrochem. Sci., 7 (2012) 1898–1907.

[21] I. Ali, V.K. Gupta, Advances in water treatment by adsorption technology, Nature Protocols, 1 (2006) 2661–2667.

[22] I. Ali, T.A. Khan, M. Asim, Removal of arsenate from groundwater by electrocoagulation method, Environ. Sci. Pollut. Res., 19 (2012) 1668–1676.

[23] I. Ali, New Generation adsorbents for water treatment, Chem. Rev., 112 (2012) 5073–5091.

[24] World Health Organisation (WHO), Guidelines for Drinking Water Quality, 1993, p. 41.

[25] K.L. Dubrawski, M. Fauvel, M. Mohseni, Metal type and natural organic matter source for direct filtration electrocoagulation of drinking water, J. Hazard. Mater., 244–245 (2013) 135–141.

[26] T.S.A. Singh, S.T. Ramesh, New trends in electrocoagulation for the removal of dyes from wastewater: a review, Environ. Eng. Sci., 30 (2013) 333–349.

[27] M. Sahana, H. Srikanth, S. Mahesh, M. Mahadeva Swamy, Coffee processing industrial wastewater treatment using batch electrochemical coagulation with stainless steel and Fe electrodes and their combinations and recovery and reuse of sludge, J. Water Sci. Technol., 78 (2018) 279–288.

[28] S. Singh, S. Mahesh, M. Sahana, K.M. Puneeth, Treatment of healthcare facility wastewaters by two dimensional (2D) electrochemical coagulation, settling and filterability aspects, J. Water Process Eng., 26 (2018) 200–220.

[29] T. Karichappan, S. Venkatachalam, P.M. Jeganathan, Optimization of electrocoagulation process to treat grey wastewater in batch mode using response surface methodology, J. Environ. Health Sci. Eng., 12 (2014) 29.

[30] P. Aswathy, R. Gandhimathi, S.T. Ramesh, P.V. Nidheesh, Removal of organics from bilge water by batch electrocoagulation process, Sep. Purif. Technol., 159 (2016) 108–115.

[31] A. Kumar, P.V. Nidheesh, M.S. Kumar, Composite wastewater treatment by aerated electrocoagulation and modified peroxi-coagulation processes, Chemosphere, 205 (2018) 587–593.

[32] R. Kamaraj, S. Vasudevan, Evaluation of electrocoagulation process for the removal of strontium and cesium from aqueous solution, Chem. Eng. Res. Design, 93 (2015) 522–530.

[33] K. Thella, B. Verma, V.C. Srivastava, K.K. Srivastava, Electrocoagulation study for the removal of arsenic and chromium from aqueous solution, J. Environ. Sci. Health, A Toxic/Hazard. Subst. Environ. Eng., 43 (2008) 554–562.

[34] S. Vasudevan, J. Lakshmi, G. Sozhan, Studies on the Al–Zn–In-alloy as anode material for the removal of chromium from drinking water in electrocoagulation process, Desalination, 275 (2011) 260–268.

[35] S. Vasudevan, J. Lakshmi, G. Sozhan, Optimization of the process parameters for the removal of phosphate from drinking water by electrocoagulation, Desal. Wat. Treat., 12 (2009) 407–414.

[36] T.S.A. Singh, S.T. Ramesh, An experimental study of CI Reactive Blue 25 removal from aqueous solution by electrocoagulation using aluminum sacrificial electrode: kinetics and influence of parameters on electrocoagulation performance, Desal. Wat. Treat., 52 (2014) 2634–2642.

[37] APHA, AWWA, WEF, Standard Methods for Examination of Water and Wastewater. 21st ed., The American Public Health Association (APHA), The American Water Works Association (AWWA) and the Water Environment Federation (WEP), (2005) USA.

[38] I. Ali, Mohd. Asim, T.A. Khan, Arsenite removal from water by electro-coagulation on zinc–zinc and copper–copper electrodes, Int. J. Environ. Sci. Technol., 10 (2013) 377–384.

[39] N. Modirshahla, M.A. Behnajadyand, S. Mohammadi-Aghdam, Investigation of the effect of different electrodes and their connections on the removal efficiency of 4-nitrophenol from aqueous solution by electrocoagulation, J. Hazard. Mater., 154 (2008) 778–786.

[40] H.A.M. Casillas, D.L. Cocke, J.A.G. Gomes, P. Morkovsky, J.R. Parga, E. Peterson, Electrocoagulation mechanism for COD removal, Sep. Purif. Technol., 56 (2007) 204–211.
[41] K. Sadeddin, A. Naser, A. Firas, Removal of turbidity and suspended solids electro-coagulation to improve feed water quality of reverse osmosis plant, Desalination, 268 (2001) 204–207.
[42] S. Mahesh, B. Prasad, I.D. Mall, I.M. Mishra, Electrochemical degradation of pulp and paper mill wastewater. Part I. COD and color removal, Ind. Eng. Chem, Res., 45 (2006) 2830–2839.
[43] J. Grimm, D. Bessarabov, R. Sanderson, Review of electro-assisted methods for water purification, Desalination, 115 (1998) 285–294.
[44] H. Bergmann, S. Koparal, The formation of chlorine dioxide in the electrochemical treatment of drinking water for disinfection, Electrochim. Acta, 50 (2005) 5218–5228.
[45] M. Arienzo, P. Adamo, J. Chiarenzelli, M.R. Bianco, A.D. Martino, Retention of arsenic on hydrous ferric oxides generated by electrochemical peroxidation, Chemosphere, 48 (2002) 1009–1018.
[46] H. Ching. T. Tanaka, M. Elimelech, Dynamics of coagulation of kaolin particles with ferric chloride, Water Res., 25 (1994) 559–569.
[47] C.H. Huang, L. Chen, C.L. Yang, Effect of anions on electrochemical coagulation for cadmium removal, Sep. Purif. Technol., 65 (2009) 137–146.
[48] M. Malakootian, N. Yousefi, The efficiency of electrocoagulation process using aluminum electrodes in removal of hardness from water, Iran. J. Environ. Health. Sci. Eng., 6 (2009) 131–136.
[49] A. Kraft, Electrochemical water disinfection: a short review, Platinum Metals Rev., 3 (2008) 177–185.
[50] IS: 10500 Indian Standard Specifications for Drinking Water, Bureau of Indian Standards, New Delhi, 1983
[51] P.V. Nidheesh, T.S.A. Singh, Arsenic removal by electrocoagulation process: recent trends and removal mechanism, Chemosphere, 181(2017) 418–432.